PARTICLE SIMULATION OF AURORAL DOUBLE LAYERS

Bruce L. Smith* and Hideo Okuda
Princeton Plasma Physics Laboratory
Princeton, New Jersey 08544, U.S.A.

ABSTRACT

We report on our work to simulate auroral double layers (DL's) with "realistic" particle-in-cell models. An early model simulated weak DL's formed in a self-consistent circuit but under conditions subject to the ion-acoustic instability. More recent work has focused on strong DL's formed when currentless jets are injected into a dipole magnetic field.

INTRODUCTION

For several years we have been simulating space plasmas using "realistic" models. These models have included both numerical MHD and particle-in-cell (PIC) codes. Here we discuss two PIC models that simulate auroral double layers (DL's).

An early analysis of DL's was performed by Block (1972). In his model four species of particles, reflecting/passing electrons/ions, were incident upon a strong ($eV >> kT$) DL. The two fluid equations, an adiabatic equation of state and Poisson's equation, led to two criteria on the drift velocities of ions and electrons incident on the high and low field sides of the DL, respectively. These are called the Bohm criteria in analogy with the similar criterion on ions in a plasma sheath (Bohm, 1949). In Block's model the drifts necessary to sustain the DL result in a net current.

Using these criteria as a recipe, one could easily simulate a DL. Such simulations only required fixed potentials at the boundaries to drive the necessary current or a floating potential (or even periodic boundary conditions) with large enough drifts (i.e., a current) to satisfy the criteria. Although these conditions permit DL's, in auroral regions, where DL's have been observed (Temerin and Mozer, 1984), such conditions may not be present.

Sato and Okuda (1980, 1981) performed a series of simulations with "more realistic" conditions. In one of these simulations they assumed:

1. $U_{drift\ e} < v_{the}$
2. $T_e >> T_i$
3. Floating self-consistent potentials.

This is the range of parameters for ion-acoustic instabilities, but avoids the large relative drifts which may cause the two-stream instability.

Their model was that of the polar region field lines in a self-consistent circuit. Initial conditions included a driving potential and an initial current. The subseuent potential and current were related by a fixed resistance consistent with the initial conditions. One of the results shown in Figure 1 was obtained for $v_{de}/v_{te} = 0.6$, $M/m = 100$,

* Now at Air Force Office of Scientific Research.

$n\lambda_D = 100$, $w_{pe}\Delta t = 0.2$. As is apparent, the simulation resulted in multiple weak ($eV \lesssim kT$) DL's about $1000\ \lambda_D$ apart and with scale lengths $\ell \sim 50\ \lambda_D$. These DL's are unstable and propagate at near the ion-acoustic velocity but recur at a rate such that approximately the same number of DL's are always present.

Hasegawa and Sato (1982) provided the mechanism for such DL's. Basically an ion hole is created which cuts off the electron current. Formation of an adjacent electron hole follows. This yields a DL which decays on the ion time scale.

Other authors have found different ways to relax the constraints imposed by the Bohm criteria. In particular, Kan and Lee (1980) concluded that the condition on the electron velocity was unnecessary if trapped electrons were present. Similarly Perkins and Sun (1981) demonstrated that even currentless DL's could exist. Incidentally, their analysis contrasts with that of Chiu and Schulz (1978) who computed the potential along a mirror magnetic field due to multiple species of ions and electrons using the condition of charge neutrality.

A recent experiment further indicated the possibility for modifying the conditions necessary for creation of DL's. Stenzel et al. (1981) conducted an experiment with a dipole B-field which reflected an incident ion beam. This experiment resulted in strong DL's for varying magnetic field strengths. These, too, were inherently current-less DL's.

The previous investigations compelled us to simulate a flowing neutral plasma injected along a (fully) dipole magnetic field. This model is meant to simulate the storm-generated flow from the reconnection region to the polar auroral regions. Of course, such a flow would cause ions and electrons of the same temperature to have different turning points. As the ions overshoot the electrons, a space charge potential could form and a DL would be present. This model then substantiates a source of energetic electrons for an aurora.

Parameters for the region through which such substorms are supposed to develop are $n = 10\text{-}1000\ cm^{-3}$, $B = 10^3\text{-}10^4\ \gamma$, and $T_e \lesssim T_i \sim 100$'s eV. These values yield $w_{pe} \sim w_{ce} \sim 10^5\text{-}10^6$ rad/s and $\beta << 1$. In this parameter regime the electrostatic approximation is appropriate (Krall and Trivelpiece, 1973).

RESULTS

Results for a one-dimensional PIC simulation with $L/\lambda_D = N_g = 1024$, $M/m = 25$, $w_{pe}\Delta t = 0.25$, and $B_{max}/B_{min} \simeq 25$ are shown. For boundary conditions we chose $V = 0$ at $z = 0$ (the "ionosphere") and using symmetry, $dV/dz = 0$ at $z = L$ (the "magnetosphere"). Figures 2a-c show the injection of plasma at approximately $0.8\ v_{the}$. As the plasma drifts into the dipole field, a double layer is evidenced by the acceleration of ions and electrons and by their relative charges at $L = 600\ \lambda_D$ for $w_{pe}\,t = 1900$ and $L = 800\ \lambda_D$ for $w_{pe}t = 2600$. One notes that the DL is unstable by the modulation (with $\lambda \sim 25\ \lambda_D$) and the fact that the DL moves at a velocity $200\ \lambda_D/700/w_{pe} = 2/7\ v_{the}$. This value is on the order of the ion-acoustic velocity.

The f-spectrum for different positions (Fig. 3) shows the presence of a mode at $w = 0.15\text{-}0.2\ w_{pe} \lesssim w_{pi}$ and at $w = 0.05\text{-}0.1\ w_{pe} << w_{pi}$. Similarly the mode structure (Fig. 4) gives wavelengths most strongly peaked at $\lambda = 0$ and $\lambda = 60\ \lambda_D$. The data are consistent with a two-stream instability (with $w << w_{pi}$). Finally the scale length of the DL is $kT/eE \sim 50\ \lambda_D >> \lambda_D$.

In the next panels (Figs. 5 a-d) are shown $f(v_+)$-$f(v_-)$ for both electrons and ions at different positions. If there were simply a B-field with no other interaction we would expect a snapshot of the loss cone for such a comparison. Instead the panels clearly show that the electrons accelerate from $w_{pe}t = 1000$ to $w_{pe}t = 2800$ as they pass over the DL. Similarly the ions slow down and cool during this same time. (This cooling of ions may allow an ion-acoustic instability.)

In the final panels (Fig. 6) we show the measured energies from the simulation. As can be seen in the first panel, total energy is conserved to within less than 1 percent. One also sees that the ion kinetic energy is converted to electron kinetic energy until the two are approximately equal. Surprisingly, the collective potential energy is a small fraction of the total.

A theory for this model was derived by Serizawa and Sato (unpublished manuscript). Using an adiabatic approximation, their kinetic analysis showed that $eV \approx KE_i/(1 + T_i/T_e)$ with small variations predicted for mass ratios $m/M << 1$ and mirror ratios $B_{max}/B_{min} >> 1$. A plot of eV versus KE_i for varying KE_i confirms the linear relation between these quantities (Fig. 7).

Similar results for ions and electrons streamed from both ends are obtained.

CONCLUSION

In conclusion, simulations have been undertaken to model aurorae under realistic conditions. The simulation of ion acoustic DL's in a self-consistent circuit showed multiple DL's with $eV/kT \lesssim 1$. Currentless DL's with $eV >> kT$ have been demonstrated. Although not discussed here, these simulations furthered the theory of Fourier transforms for bounded systems and successfully demonstrated the utility of a guiding center code for electrons. Currently two-dimensional codes are being tested to verify the one-dimensional results and to study two-dimensional instability mechanisms.

REFERENCES

Block, L. P., *Cosmic Electrodynamics, 3,* 349 (1972).

Bohm, D., in *The Characteristics of Electrical Discharges in Magnetic Fields,* edited by A. Guthrie and R. K. Wakerling, p. 77, McGraw-Hill, New York, 1949.

Chiu, Y. T., and M. Schulz, *J. Geophys. Res., 83,* 629 (1978).

Hasegawa, A., and T. Sato, *Phys. Fluids, 25,* 632 (1982).

Kan, J. R., and L. C. Lee, *J. Geophys. Res., 85,* 788 (1980).

Krall, N. A., and A. W. Trivelpiece, in *Principles of Plasma Physics,* p. 427, McGraw-Hill, New York, 1973.

Perkins, F. W., and Y. C. Sun, *Phys. Rev. Lett., 46,* 115 (1981).

Sato, T., and H. Okuda, *Phys. Rev. Lett., 44,* 740 (1980).

Sato, T., and H. Okuda, *J. Geophys. Res., 86,* 3357 (1981).

Serizawa, Y., and T. Sato, unpublished report on "Generation of Large Scale Potential Difference by Currentless Plasma Jets Along the Mirror Field."

Stenzel, R. L., M. Ooyama, and Y. Nakamura, *Phys. Fluids, 24,* 708 (1981).

Temerin, M., and F. Mozer, in *Second Symposium on Plasma Double Layers and Related Topics,* edited by R. Schrittwieser and G. Eder, p. 119, University of Innsbruck, 1984.

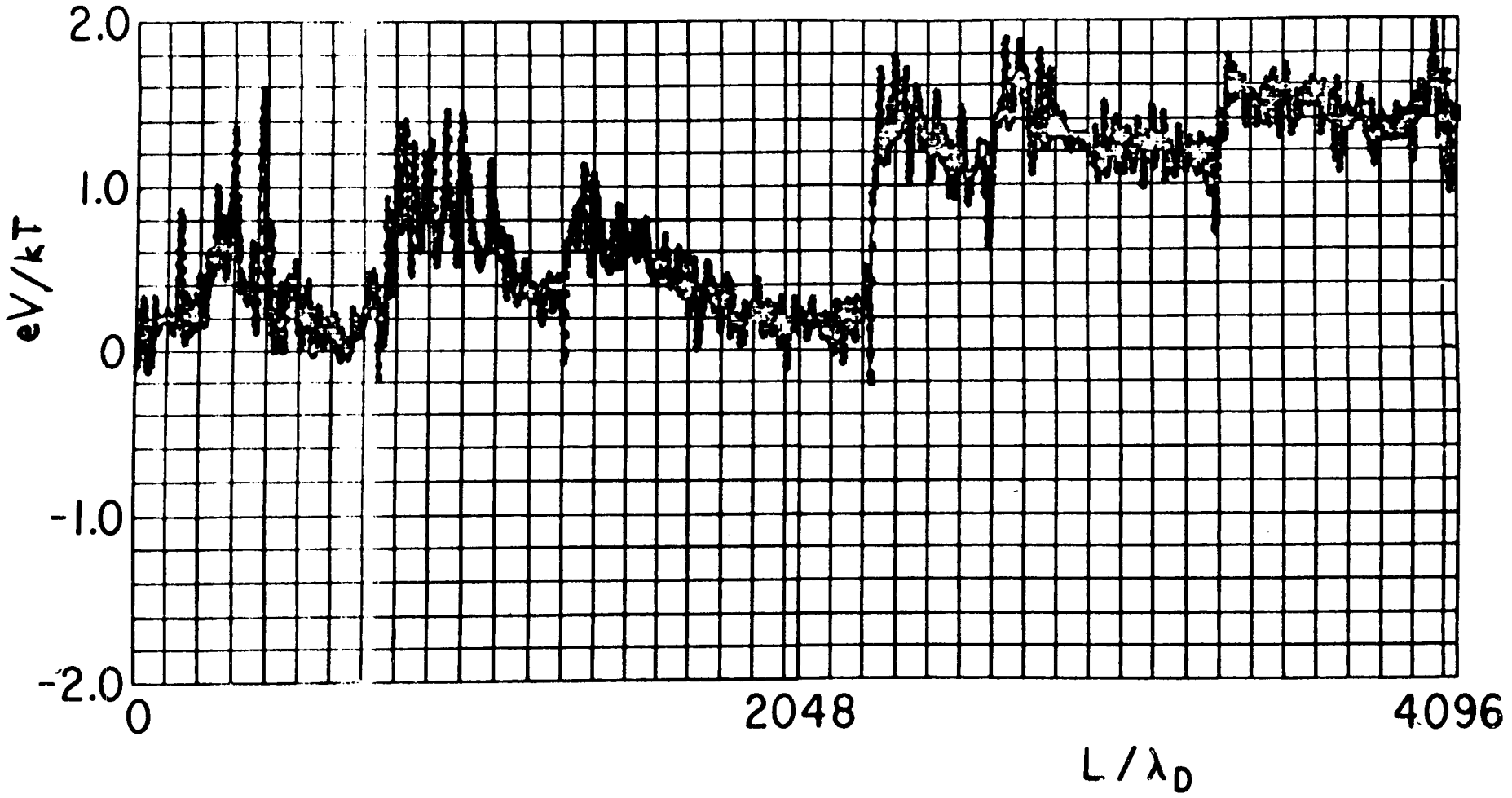

Figure 1. The electric potential as a function of position showing the formation of multiple weak double layers. The simulation results here are due to Sato and Okuda (1980, 1981).

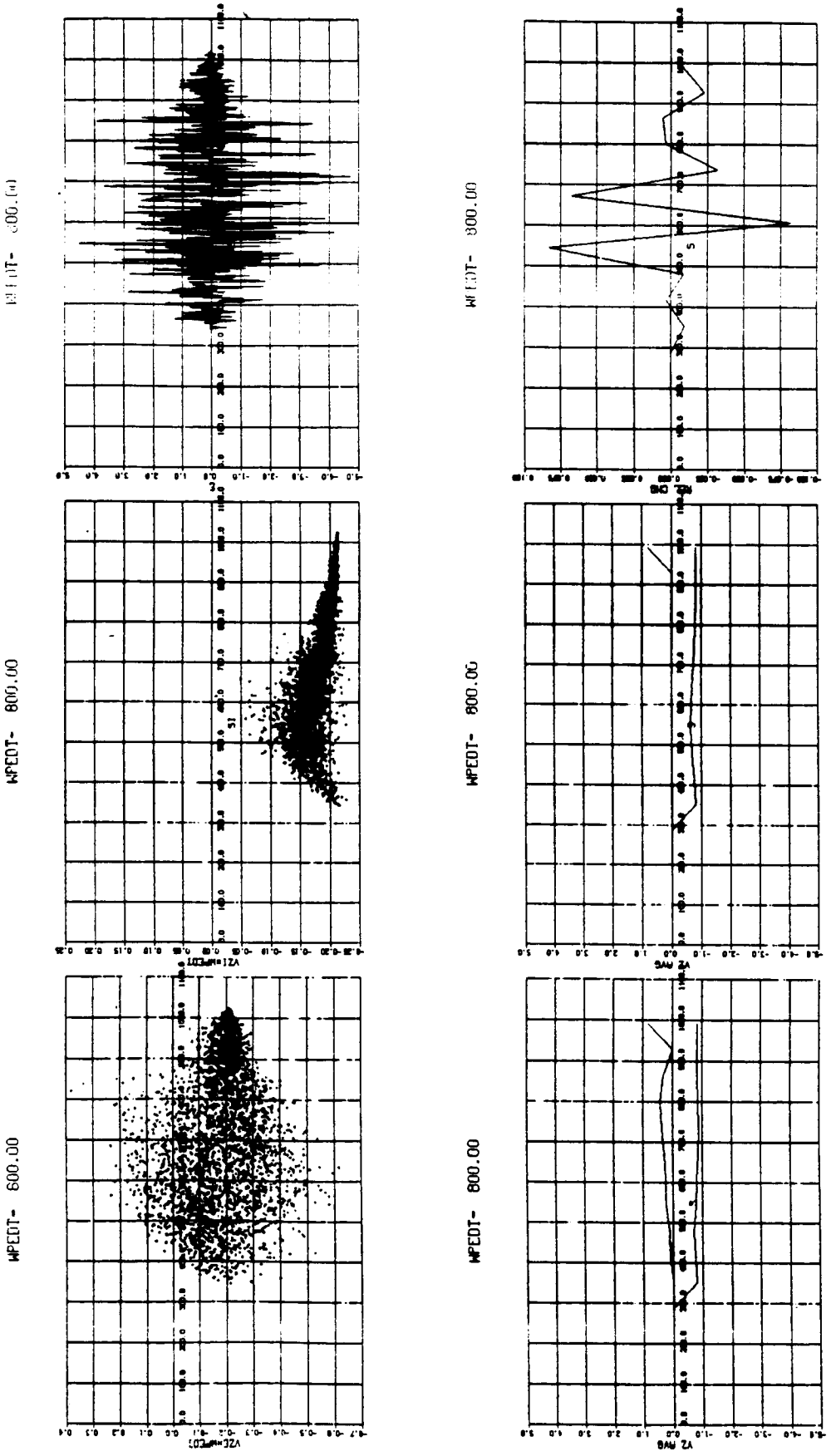

Figure 2. Results for a one-dimensional simulation with $L/\lambda_0 = Ng = 1024$, $M/m = 25$ $B_{max}/B_{min} \simeq 25$, and $w_{pe}\Delta t$ as indicated by the value of WPEDT in the figures.

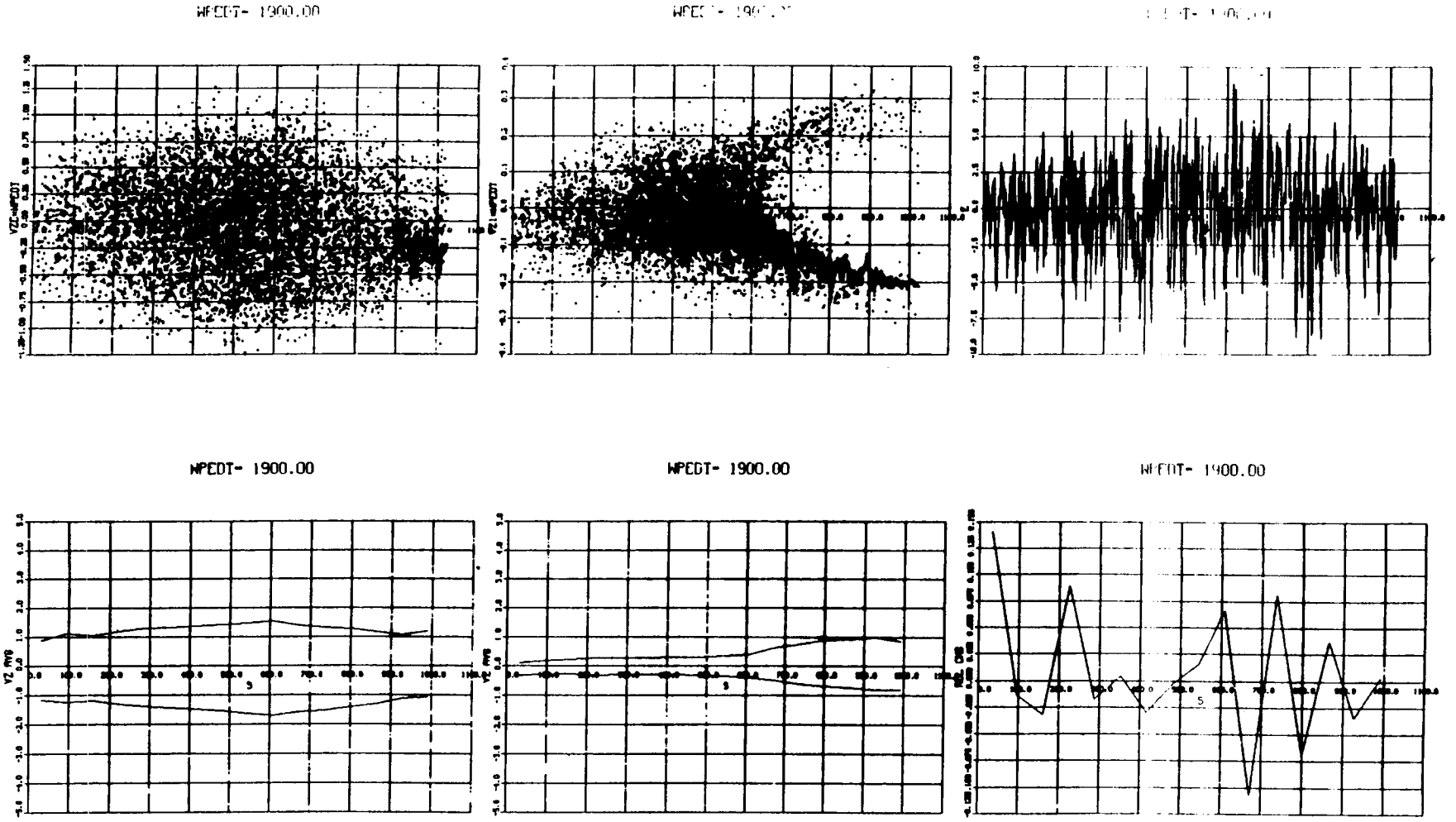

Figure 2. (Continued)

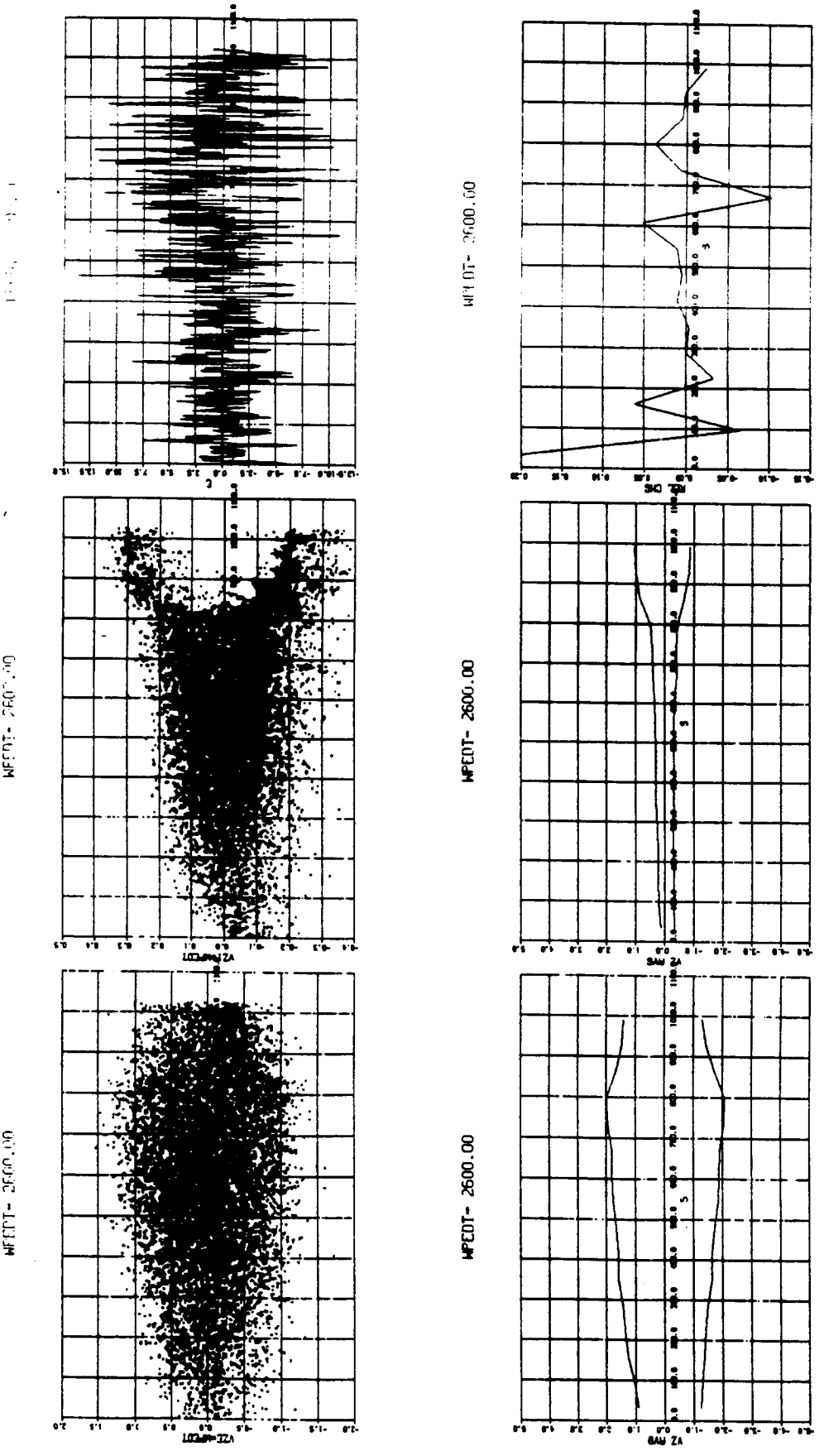

Figure 2. (Concluded)

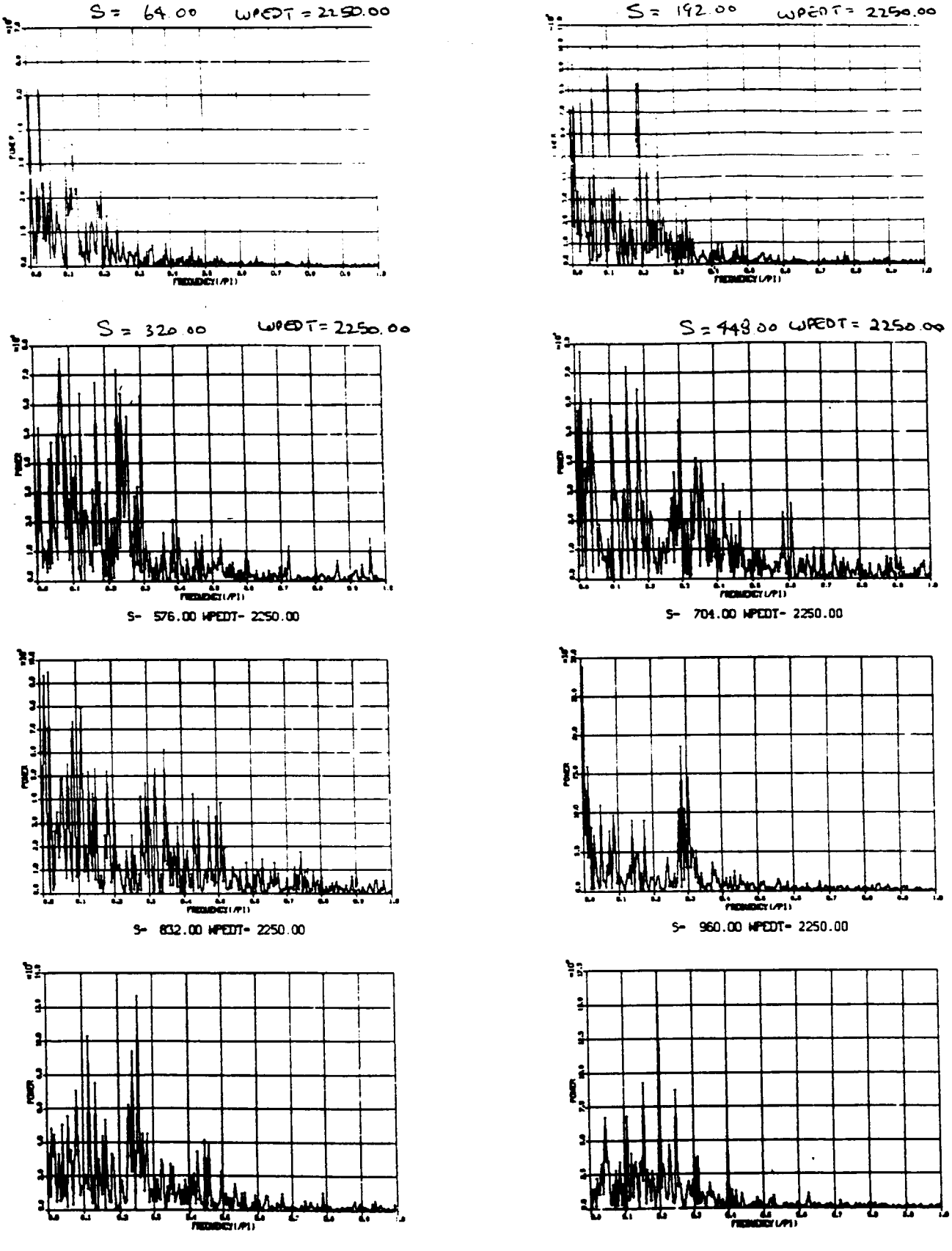

Figure 3. The frequency spectrum for different positions with $w_{pe}\Delta t = 2250$.

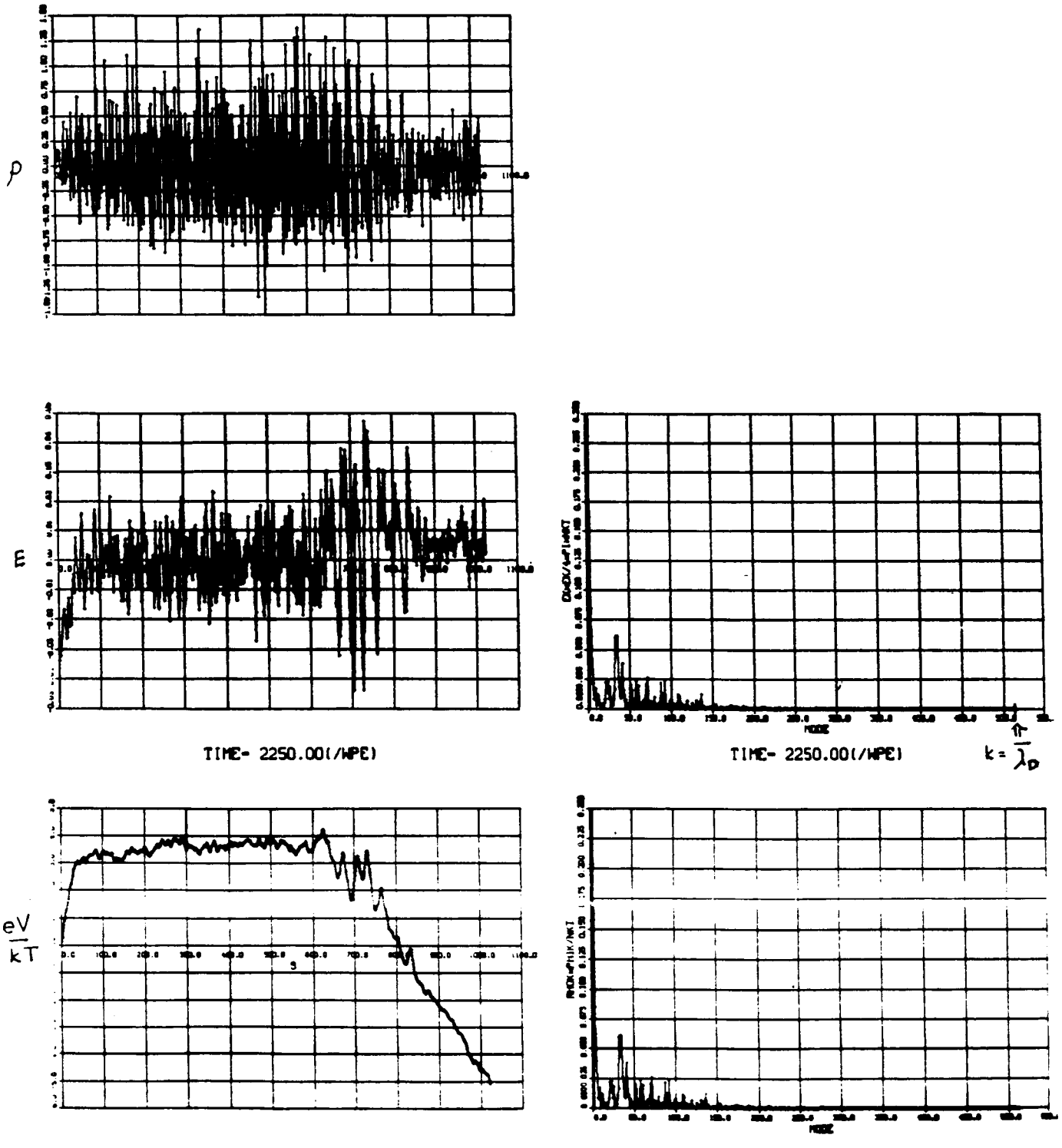

Figure 4. The charge density, electric potential, electric field intensity, and mode structure from the simulations of Figure 3.

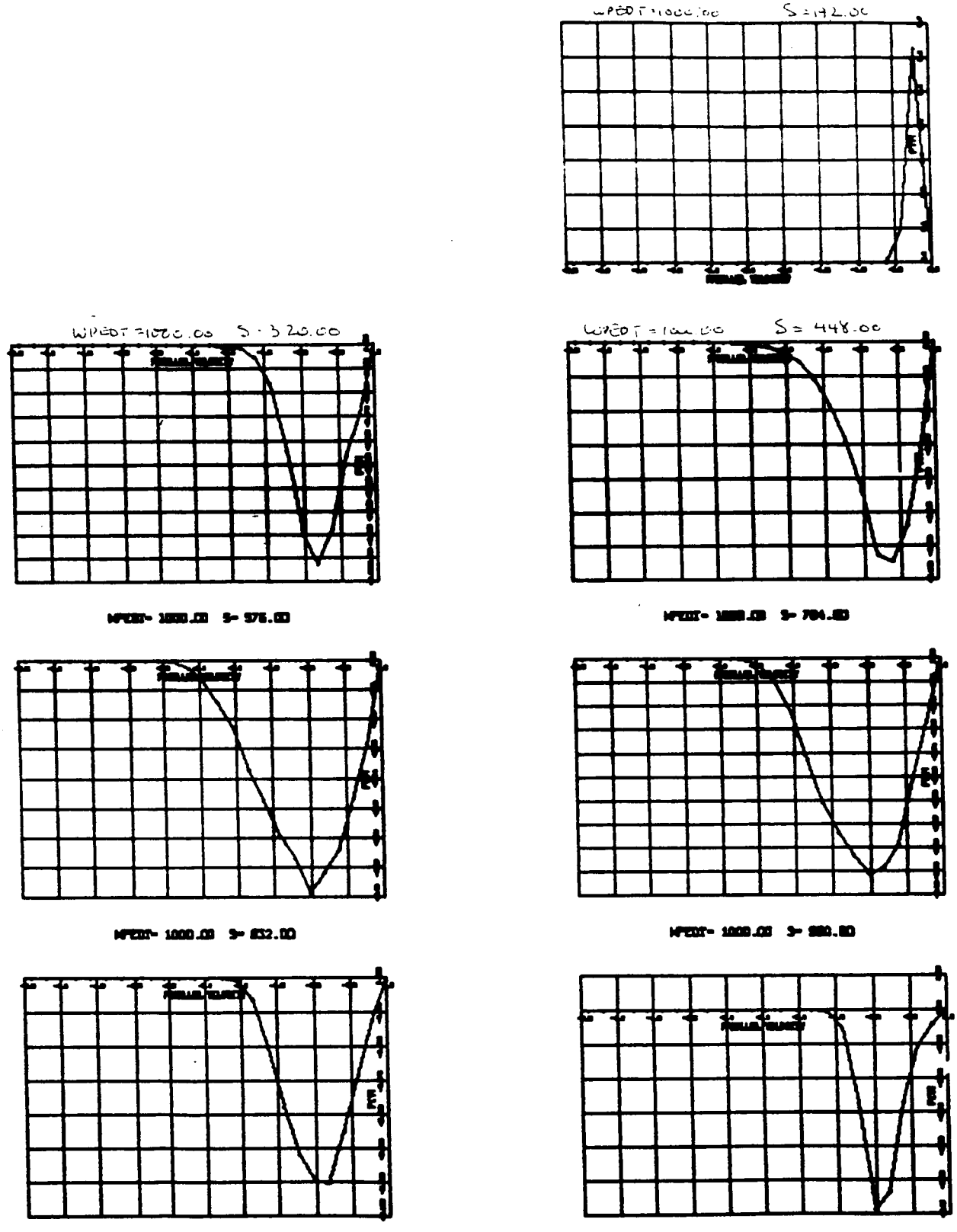

(a)

Figure 5. A plot of $f(v_+) - f(v_-)$ for the electrons and ions at various positions.

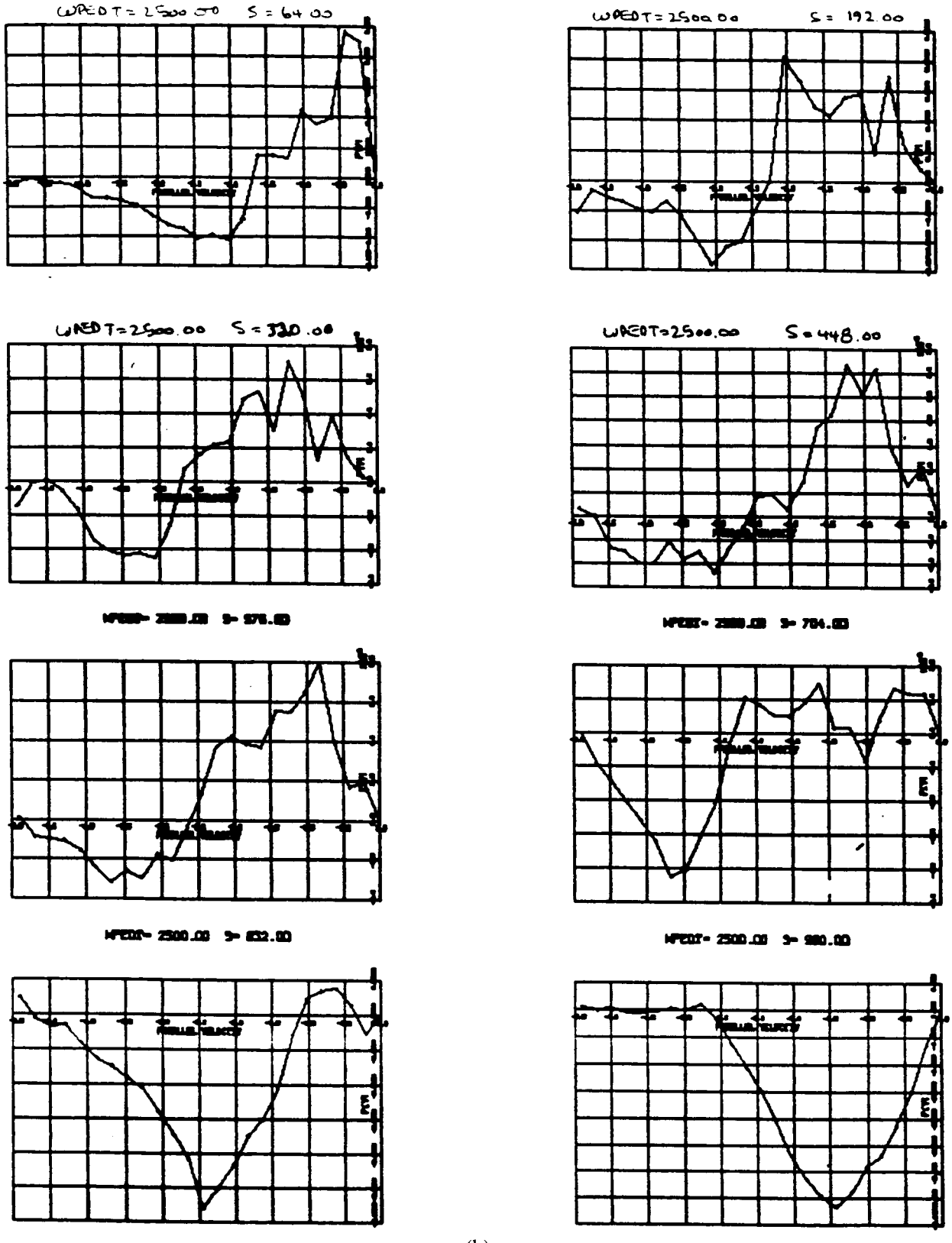

(b)

Figure 5. (Continued)

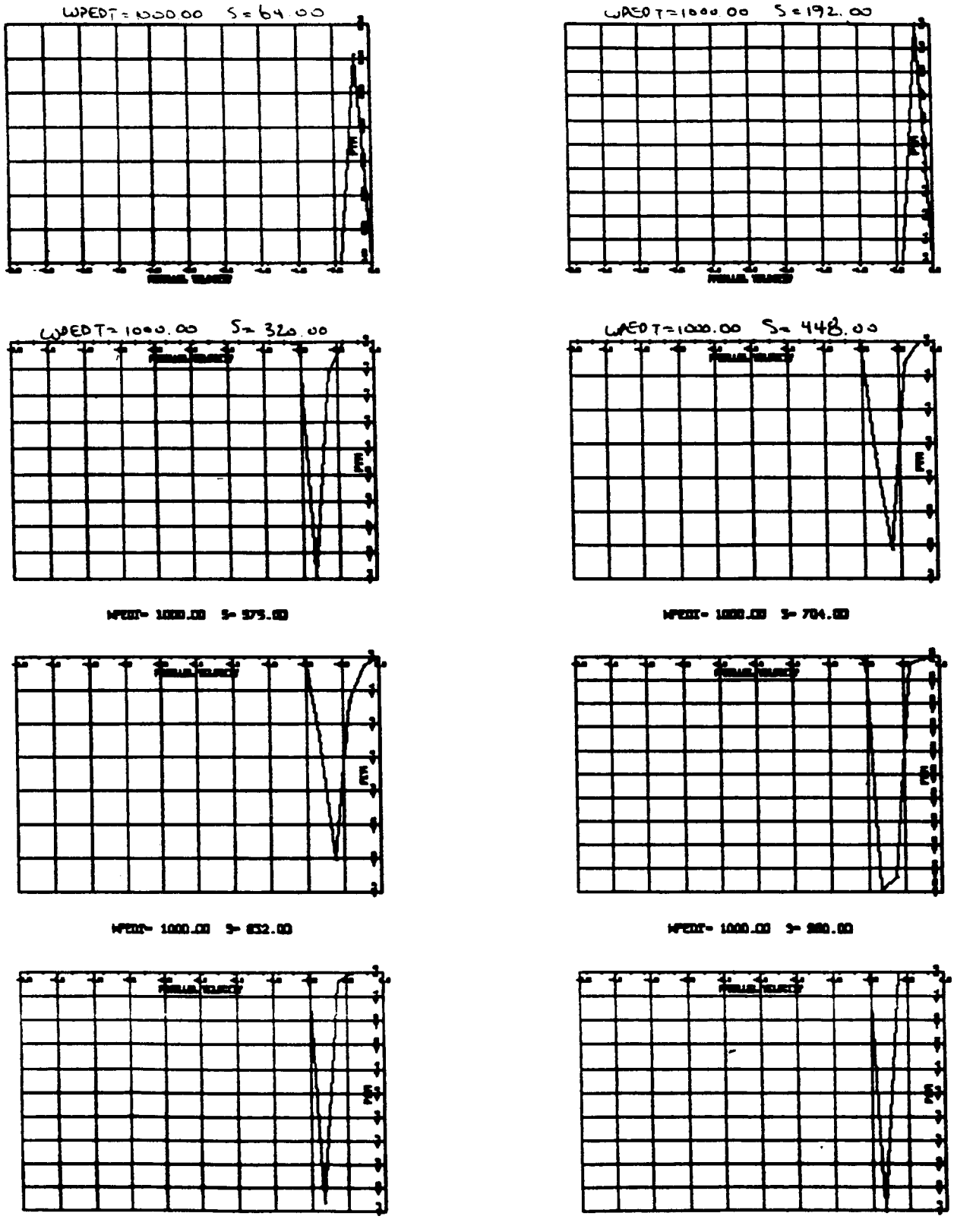

(c)

Figure 5. (Continued)

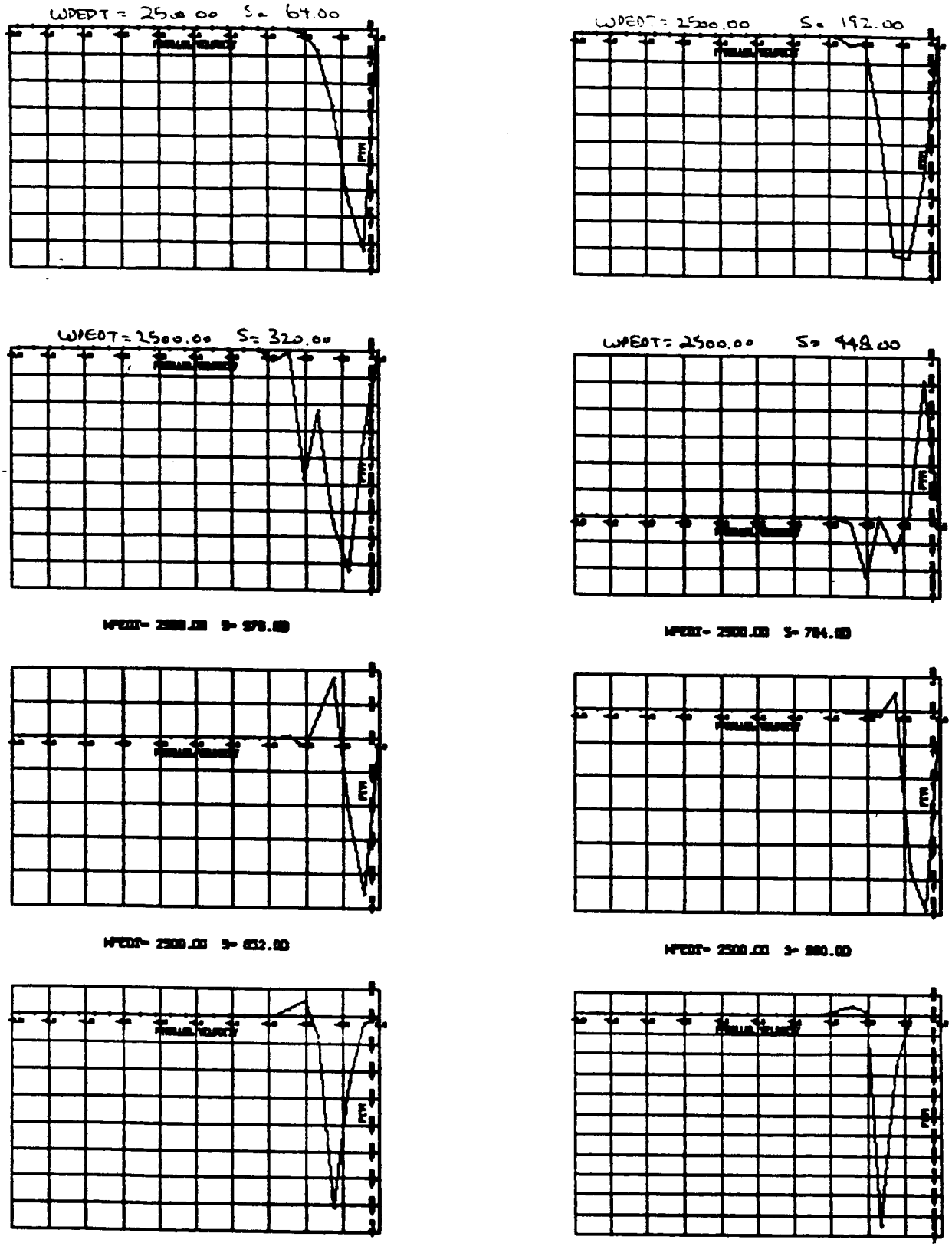

(d)

Figure 5. (Concluded)

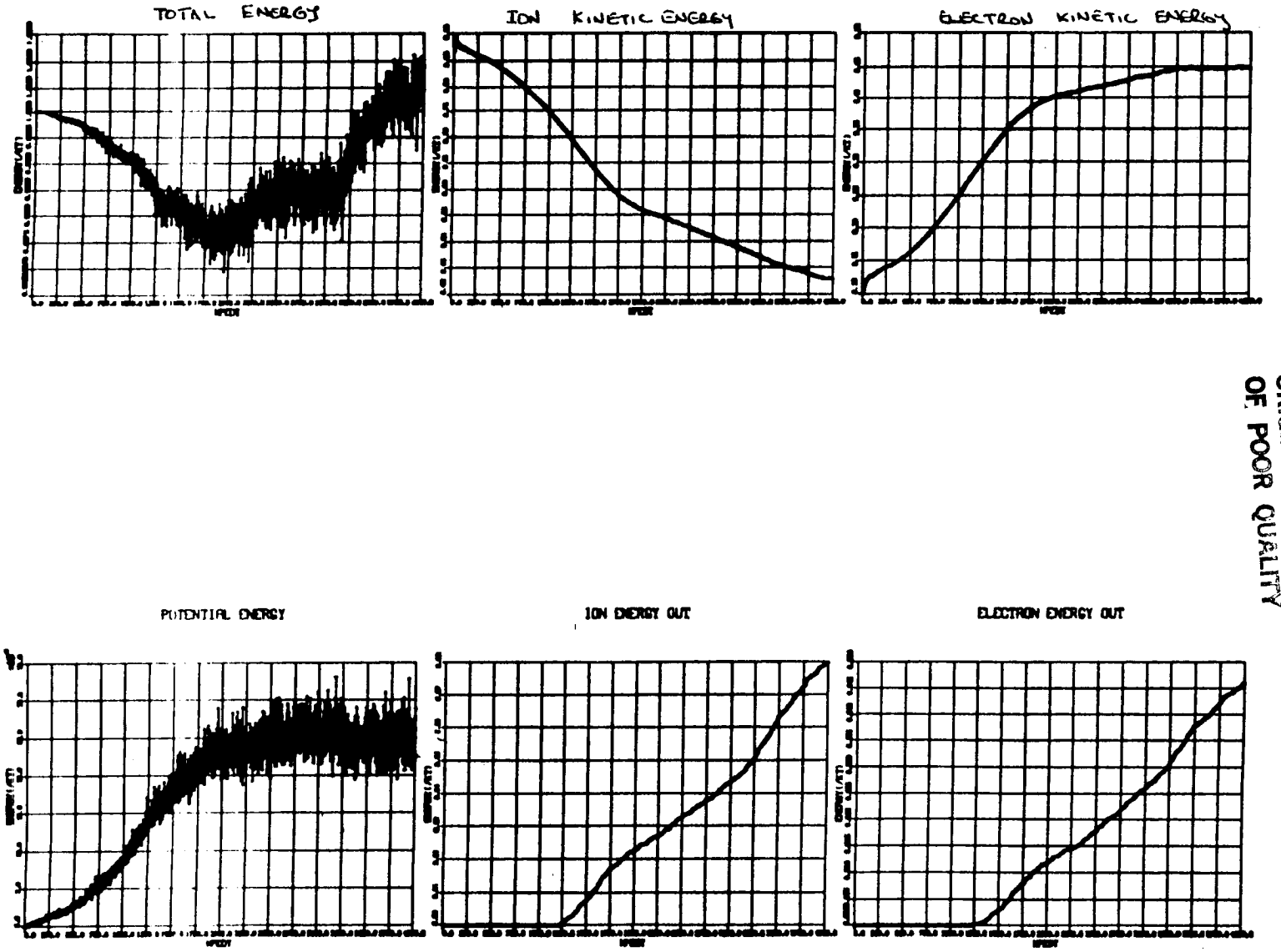

Figure 6. The calculated energies implicit in the simulation results.

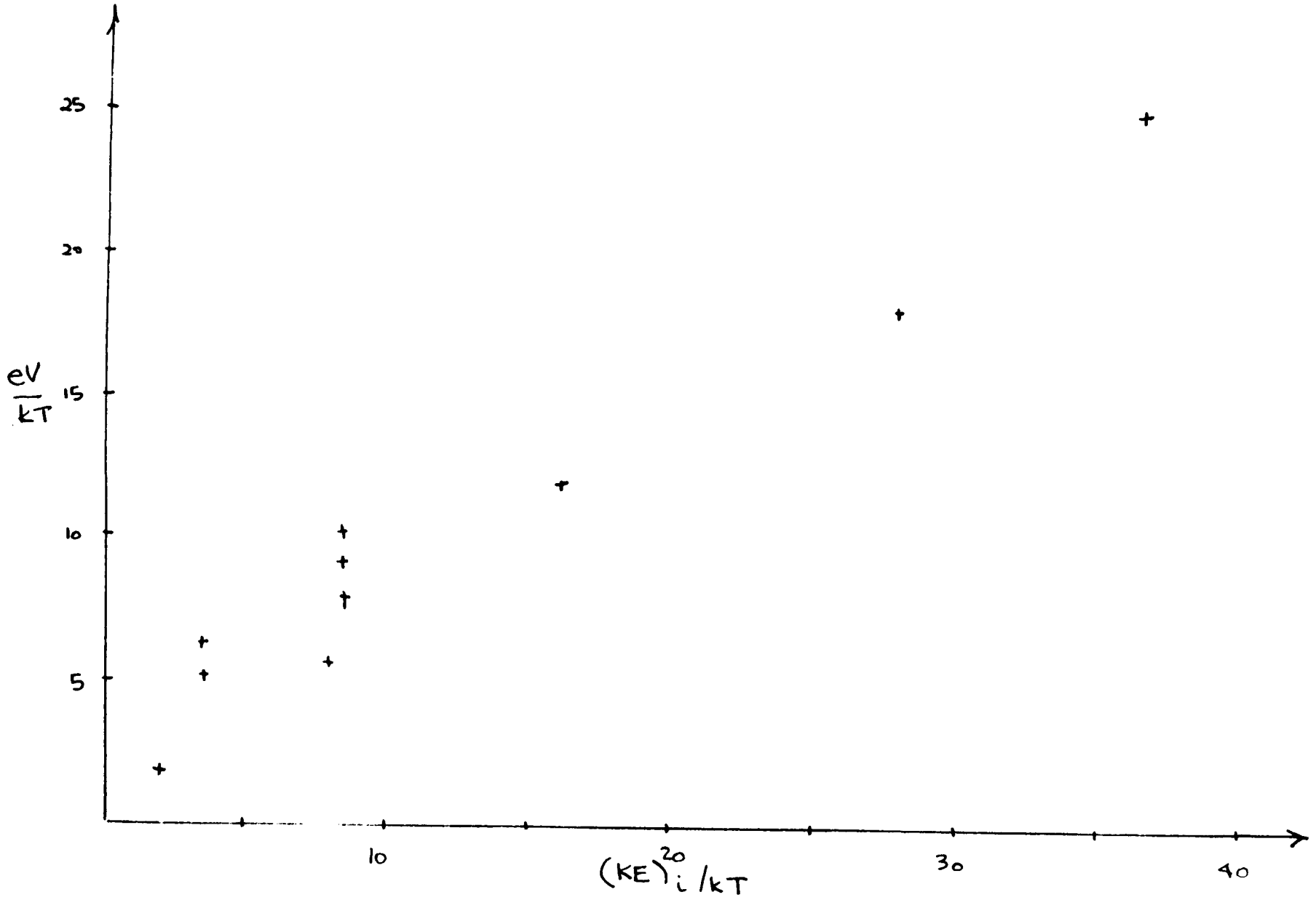

Figure 7. A plot of the double layer potential eV versus the ions kinetic energy.